IL NUOVO CIMENTO Vol. 31 C, N. 3 Maggio-Giugno 2008
DOI 10.1393/ncc/i2008-10296-2

Dynamic behaviour of lagoon ecosystems

F. Cioffi(*)

Dipartimento di Idraulica, Trasporti e Strade, Università di Roma "La Sapienza"
Via Eudossiana 18, 00184, Rome, Italy

(ricevuto il 22 Settembre 2008; revisionato il 26 Novembre 2008; approvato il 27 Novembre 2008; pubblicato online il 13 Gennaio 2009)

Summary. — The dynamic behaviour of primary producers in coastal lagoons due to changes of external control parameters—phosphorous external load and maximum tidal flow rate—is investigated by using a eutrophication model. The eutrophication model allows the simulation of the temporal evolution of the concentration of the following species: a) in the water column: dissolved oxygen, vegetal organic carbon, particulate and dissolved organic carbon, dissolved phosphorous and hydrogen sulphide; b) in sediments: dissolved oxygen, particulate and dissolved organic carbon, dissolved and adsorbed phosphorous, hydrogen sulphide. The vegetal organic carbon is distinguished in three components related to the main groups of primary producers, namely eelgrass, macroalgae and microalgae, having different modalities of nutrient uptake and kinetics parameters depending on the S/V ratio. Diagrams representing the ecosystem dynamic response to the changes of the control parameters were constructed by simulations. The response diagrams suggest the existence of regime shifts which border different ecosystem stability ranges, characterized by the dominance of a specific group of primary producers and by different ecosystem vulnerability at summer water anoxia. A catastrophic bifurcation or abrupt regime shift—evidenced by Poincarè sections obtained mapping, at a prefixed time period, the values of the concentration of the species—occurs for a critical value of the control parameter and manifests itself as an abrupt change of the dominant species from eelgrass to macroalgae. An analogous abrupt change from eelgrass to macroalgae occurs for a critical value of the tidal flowrate assumed as control parameter in simulations conducted for an assigned value of external phosphorous load.

PACS 92.20.jm – Population dynamics and ecology.
PACS 92.20.jp – Ecosystems, structure, dynamics and modelling.
PACS 92.20.ju – Nutrients and nutrient cycling.
PACS 92.40.qn – Ponds.

(*) E-mail: francesco.cioffi@uniroma1.it

1. – Introduction

One of the most evident effects of eutrophication in coastal lagoons is the change, in the long run, in vegetable species with reduction of diversity and prevalence of infesting species; such change is also accompanied by an increase of the summer water anoxia vulnerability of the lagoons and fish kills.

Recent investigations have shown that a correlation exists between the lagoon eutrophication levels, vulnerability to water anoxia and type of dominant vegetable species: coastal lagoons having lower eutrophication levels, in which summer water anoxia events are rare or absent, are mainly colonised by rooted species (as eelgrass), while in highly eutrophic environments, in which more frequently water anoxia phenomena occur, different floating species, from macroalgae to microalgae, are dominant [1-6].

There is a strong and complicate cause-effect link between eutrophication trend on the long run, kind of dominant primary producers and instantaneous conditions leading to summer water anoxia. In fact, growth of high quantity of aquatic vegetation (as a consequence of eutrophication) and summer anoxia have a mutual relation, because high quantities of vegetation produce proportional organic detritus quantities which accumulates into sediments; the aerobic mineralisation of organic detritus in sediments induces considerable dissolved oxygen consumption; if the oxygen flows from the atmosphere to water column and to sediments, due to the turbulence intensity (depending on the instantaneous lagoon hydrodynamic conditions) are not sufficient to compensate the mineralisation consumption of dissolved oxygen, anoxic conditions are reached in sediments. In such conditions both adsorbed phosphorous and hydrogen sulphide are release into the water column. The first produces an increase in orthophosphate concentration in water which stimulates the further vegetal growth (worsening the eutrophication conditions), while the second, due to the re-oxidation of hydrogen sulphide, accelerates the dissolved oxygen consumption into the water column leading to water anoxia. The described phenomena, affecting the eutrophication trend on the long term of a lagoon, depend on both the hydrodynamic behaviour of water body (due to lagoon morphology, and to entity of the forcing factors tide and wind), and the characteristics of the dominant vegetal species into the lagoon: life cycle, organic detritus production and nutrient uptake. It should be noted that the described phenomena are further on made complicated because the dominant vegetal species in a lagoon do not remain the same in each case but they can change as a consequence of variations of climatic and hydrodynamic factors or of external nutrient loads.

Therefore lagoon ecosystems exhibit very complex dynamics which is due to nonlinear interactions of biological, chemical and hydrodynamic processes that influence the cycles of carbon (vegetal growth, organic detritus production and mineralization), nutrients, sulphur, and of all those species playing any role in ecological phenomena [7-10]. Such a dynamic is influenced by various external forcing variables—tidal flow rate, wind speed, temperature, light intensity, nutrient external load—that in most of the cases are periodical or multi-periodical. Anthropogenic or natural changes in one or more of these external variables can trigger shifts between ecosystem states which can be evidenced by species composition shift, higher vulnerability of the lagoon to summer water anoxia, more frequent fish kills. These regime shifts can be smooth, abrupt or discontinuous; furthermore they may not be immediately reversible [11, 12].

The understanding of the mechanisms driving the regime shifts, *i.e.* of the cause-effect link between eutrophication trend on the long run, type of dominant vegetal species, and instantaneous conditions leading to summer water anoxia, appears to be fundamental to individuate strategies to management lagoon ecosystems.

In this paper the ecosystem dynamic in lagoons, as a consequence of nutrient enrichment, was investigated by a more extended version of the eutrophication model proposed by Cioffi and Gallerano [13, 14]. The rate of phosphorous external load was assumed as control parameter. Diagrams representing the ecosystem dynamic response to the changes of the control parameter were constructed by simulations. The response diagrams suggest the existence of regime shifts which border different ecosystem stability ranges, characterized by the dominance of a specific group of primary producers and by different ecosystem vulnerability at summer water anoxia. A catastrophic bifurcation or abrupt regime shift—evidenced by Poincarè sections obtained mapping, at a prefixed time period, the values of the concentration of the species—occurs for a critical value of the control parameter and manifests itself as an abrupt change of the dominant species from eelgrass to macroalgae. An analogous abrupt change from eelgrass to macroalgae occurs for a critical value of the tidal flowrate assumed as control parameter in simulations conducted for an assigned value of external phosphorous load.

2. – Hypothesis and model equations

The model simulates, in water column and in sediments, the concentration temporal evolution of the species: dissolved oxygen, vegetal organic carbon, particulate and dissolved organic carbon, orthophosphate, hydrogen sulphide, adsorbed phosphorous.

In order to limit the computation times needed for the large number of simulations required for the analysis of ecosystem dynamics, the model is applied to a hypothetical and schematic lagoon, having superficial area A, tidal flow rate q, and a constant depth h. However, the two main hydrodynamic effects on eutrophication processes—turbulent diffusion and flushing of the species from the lagoon toward the sea—are represented respectively by vertical turbulent diffusion terms (whose turbulent diffusion coefficient is related to the instantaneous value of tidal flow rate and wind speed [13])—and sink/source terms related to the tidal flow rate and to the volume of the lagoon.

The mass balance equations of the model are the following:

$$\begin{aligned}(1)\qquad \frac{\partial C_{al}}{\partial t} &= \frac{\partial}{\partial z}\left(\nu_t \frac{\partial C_{al}}{\partial z}\right) + \begin{pmatrix}\mu_{cral}\cdot f_a(P_o)\cdot f(I)\cdot f_{al}(T) - r_{al} f_{al}(T) - \\ -\frac{K_{dal}}{f_{al}(T)} - \frac{K_{pal}}{f_{al}}(T)\end{pmatrix}\cdot C_{al} \\ &\quad +\alpha_{al}\cdot (q/(A\cdot h))\cdot \sin(\omega_m t)\cdot \tilde{C}_{al},\end{aligned}$$

$$\begin{aligned}(2)\qquad \frac{\partial C_{ph}}{\partial t} &= \frac{\partial}{\partial z}\left(\nu_t \frac{\partial C_{ph}}{\partial z}\right) \\ &\quad +\Bigg(\mu_{cph}\cdot f_{ph}(P_o)\cdot f(I)\cdot f_{ph}(T) \\ &\qquad -r_{ph} f_{ph}(T) - \frac{K_{dph}}{f_{ph}(T)} - \frac{K_{pph}}{f_{ph}(T)}\Bigg)\cdot C_{ph} \\ &\quad +(q/(A\cdot h))\cdot \sin(\omega_m t)\cdot \tilde{C}_{ph},\end{aligned}$$

$$\begin{aligned}(3)\qquad \frac{\mathrm{d}\tilde{C}_m}{\mathrm{d}t} &= \int_o^h \Bigg(\mu_{crm}\cdot f_s(P_o, P_{ads})\cdot f(I)\cdot f_m(T) \\ &\qquad -r_m\cdot f_m(T) - \frac{K_{dm}}{f_m(T)} - \frac{K_{pm}}{f_m(T)}\Bigg)\cdot C_m \mathrm{d}z,\end{aligned}$$

$\tilde{C}_m = \int_0^h C_m(z)\mathrm{d}z$ with $C_m(z) < C_{\max}$,

$$\begin{aligned}(4)\qquad \frac{\partial C_d}{\partial t} &= \frac{\partial}{\partial z}\left(\nu_t \frac{\partial C_d}{\partial z}\right) + \frac{K_{dal}}{f_{al}(T)} \cdot C_{al} + \frac{K_{dm}}{f_m(T)} \cdot C_m \\ &\quad + \frac{K_{dph}}{f_{ph}(T)} \cdot C_{ph} - \mu_d \cdot f_\mu(T) \cdot f(C_d) \cdot f(O_2) \\ &\quad + K_p C_p \alpha_{por} - K_s C_d + (q/(A \cdot h)) \cdot \sin(\omega_m t) \cdot \tilde{C}_d + q_{dmm},\end{aligned}$$

$$\begin{aligned}(5)\qquad \frac{\partial C_p}{\partial t} - v_s \frac{\partial C_p}{\partial z} &= \frac{\partial}{\partial z}\left(\nu_t \frac{\partial C_p}{\partial z}\right) - K_p C_p + \frac{K_{pal}}{f_{al}(T)} \cdot C_{al} + \frac{K_{pm}}{f_m(T)} \cdot C_m \\ &\quad + \frac{K_{pph}}{f_{ph}(T)} \cdot C_{ph} + (q/(A \cdot h)) \cdot \sin(\omega_m t) \cdot \tilde{C}_p + q_{pimm},\end{aligned}$$

$$\begin{aligned}(6)\qquad \frac{\partial P_o}{\partial t} &= \frac{\partial}{\partial z}\left(\nu_t \frac{\partial P_o}{\partial z}\right) + K_{pc}(\mu_d f_\mu(T) f(C_d) f(O_2) + K_s C_d) \\ &\quad - K_{pc}(\mu_{cral} f_a(P_o) f(I) f_{al}(T) - r_{al} f_{al}(T)) \cdot C_{al} \\ &\quad - K_{pc}\big(\mu_{cph} \cdot f_{ph}(P_o) \cdot f(I) \cdot f_{ph}(T) \\ &\qquad - r_{ph} f_{ph}(T)\big) \cdot C_{ph} - \frac{1 - p_{or}}{p_{or}} \cdot K_a(P_{ae} - P_a) \\ &\quad + \alpha_p \left(\frac{1 - p_{or}}{p_{or}}\right) - \big[\mu_{crm} \cdot f_s(P_o, P_{ads}) \cdot f(I) \cdot f_m(T) \\ &\qquad - f_m(T) \cdot r_m\big] \cdot \frac{\tilde{C}_m K_{pmc}}{h_s} \cdot f'(z) \\ &\quad + (q/(A \cdot h)) \cdot \sin(\omega_m t) \cdot \tilde{P}_o + q_{poimm},\end{aligned}$$

$$\begin{aligned}(7)\qquad \frac{\mathrm{d}P_a}{\mathrm{d}t} &= K_a(P_{ae} - P_a) - \alpha_p - \Big(\mu_{crm} \cdot f_s(P_o, P_a) \cdot f_m(I) \cdot f_m(T) \\ &\qquad - f_m(T) \cdot r_m\Big) \cdot \frac{\tilde{C}_m K_{pmc}}{h_s} \cdot f''(z),\end{aligned}$$

$$(8)\qquad \frac{\partial H}{\partial t} = \frac{\partial}{\partial z}\left(\nu_t \frac{\partial H}{\partial z}\right) - K_H OH + \alpha_s \cdot K_s C_d + (q/(A \cdot h)) \cdot \sin(\omega_m t) \cdot \tilde{H},$$

$$\begin{aligned}(9)\qquad \frac{\partial O}{\partial t} &= \frac{\partial}{\partial z}\left(\nu_t \frac{\partial O}{\partial z}\right) + \alpha_\mu \cdot \Big(\mu_{cph} \cdot f_{ph}(P_o) \cdot f(I) \cdot f_{ph}(T) \\ &\qquad - r_{ph} f_{ph}(T) - \frac{K_{dph}}{f_{ph}(T)} - \frac{K_{pph}}{f_{ph}(T)}\Big) \cdot C_{ph} \\ &\quad + \alpha_\mu \cdot \Big(\mu_{cral} \cdot f_a(P_o) \cdot f(I) \cdot f_{al}(T) - r_{al} \cdot f_{al}(T) \\ &\qquad - \frac{K_{dal}}{f_{al}(T)} - \frac{K_{pal}}{f_{al}(T)}\Big) \cdot C_{al} \\ &\quad + \alpha_\mu \cdot \Big(\mu_{crm} \cdot f_s(P_o, P_a) \cdot f(I) \cdot f_m(T) \\ &\qquad - r_m \cdot f_m(T) - \frac{K_{dm}}{f_m(T)} - \frac{K_{pm}}{f_m(T)}\Big) \cdot C_m - \beta_1 \cdot \mu_d f_\mu(T) \\ &\quad \cdot f(C_d) \cdot f(O_2) - \beta_2 K_H OH + \alpha_o(q/(A \cdot h)) \cdot \sin(\omega t) \cdot \tilde{O}.\end{aligned}$$

The meaning of the symbols of eqs. (1)-(9) is reported in appendix. Equations (1)-(3) refer to the three main groups of primary producers [10]—eelgrass C_m (as Zostera), macro-algae C_{al} (as Ulva) and micro-algae or phytoplankton C_{ph} (as Chlorella)—whose vegetal growth, by photosynthesis, is controlled by environmental factors (light, temperature, lagoon hydrodynamics) and by the physiological characteristics of the particular vegetal species; the three species differ respect to nutrient uptake, growth and organic detritus production rates. The eelgrass (as Zostera) is a rooted vegetal species, while the other two are floating ones; eelgrass assimilates phosphorous mainly by root-rhizomes from the interstitial water of the sediment [7] and it grows starting from the bottom of the water column, then the vegetation extends to the upper layers of the water column once a maximum vegetal concentration ($C_{\max}$ in eq. (3)) is reached in the lower layers. Floating species uptake phosphorous in the water column and they grow mainly near the free surface of the water column where there are more favourable light conditions. In eqs. (1)-(3) the nutrient uptake is represented by Michaelis-Menten kinetics, $V = V_{\max}(P/(P+K_s))$, where V is the uptake velocity, $V_{\max}$ the maximum uptake velocity (which directly related to the algae growth rate), P the concentration of nutrient and K_s the half-saturation constant. Low values of K_s are thought to express a competitive advantage for algal species at low nutrient concentrations, whilst those algae with higher values of $V_{\max}$ are considered to be favoured at higher concentrations. Experimental studies in aquatic ecosystems [15] have shown that both the values of $V_{\max}$ and K_s depend on the algae size (or by surface/volume ratio, S/V): the maximum PO_4 uptake small algae capacity per unit volume is higher than large algae one, whereas K_s decreases with increasing algae size. The rate of production of organic detritus by rooted plants is lower than in floating species and it has appreciable values only at the end of the eelgrass life cycle; on the contrary the floating species, having a quickly turn over, during the entire life cycle, show a greater and more uniform detritus production rates. These rates increase with increasing of algae S/V ratio. On the basis of these observations the vegetal growth rates, the organic detritus production rates and the half-saturation constant were related to the S/V ratio [8]. Equations (4), (5) represent the mass balances, in water and sediments, of both dissolved C_d and particulate organic detritus C_p; in eqs. (4), (5) different processes are represented: vegetal organic detritus production, transformation of C_p in C_d, settling, aerobic and anaerobic mineralization. Equations (6), (7) represent the dissolved phosphorous (P_o) mass balance, in water and in sediments, and the adsorbed phosphorous (P_a) mass balance in sediments. The following processes are represented: aerobic and anaerobic adsorbing-desorbing of dissolved phosphorous in sediments, phosphorous uptakes by vegetal species, source of phosphorous by aerobic and anaerobic mineralization. Equation (8) represents the mass balance of sulphide (H) produced by anaerobic mineralization processes (sulphide reduction) and consumed by re-oxidation. Equation (9) represents the dissolved oxygen (O) mass balance as a consequence of photosynthesis, algal respiration, aerobic mineralization, sulphide re-oxidation.

Periodical forcing terms appear into the model equations. They represent the influences of external variables—as light, temperature, tidal flow rate, breeze speed—having some typical periodicity or multi-periodicity: light and temperature have both seasonal and daily variation, tidal flow rate has a semi-daily variation, and breeze speed has a daily variation.

Semi-discretization of the diffusive terms in eqs. (1)-(9) in the space variable z, on discrete points along the vertical, by using a centered finite difference scheme, yields a nN ODE system, n being the number of points of the grid and N the species number. A non-equidistant grid, obtained by applying a cosine function and having 11 points in

the water column and 6 into the sediment layer, was used in order to obtain a better approximation of the derivates close to the interface air-water and water-sediment. Because the lagoon depth h changes due to the incoming and going out tidal flow rates, the spatial grid was calculated again at each time step.

The ODE system, for assigned boundary conditions (see [13, 14]), was solved using a forth-order Runge-Kutta method. In order to implement such a method, a fortran code was constructed. A time step equal to 100 s was used in the simulations.

3. – Procedure and results

In order to analyze the response of the ecosystems, in terms of dynamic behaviour of primary producers, to the variations of nutrient load discharged in the lagoon and maximum tidal flow rate at the mouth connecting the lagoon to the sea, and further to investigate on the relationship between summer water anoxia phenomena and eutrophication state of the lagoon, the following procedure was carried out:

a) First a set of biological, chemical and physical parameters (on the basis of literature) and external forcing variables was selected; the parameter values, which define the parameter space, are reported in appendix.

b) The phosphorous load q_{poimm} ($\mathrm{g/m^3\,s}$) was assumed as control parameter whose value has been changed within a prefixed range.

c) For each selected value of the control parameter a simulation by model was carried out as long as periodic solutions of the equation system were reached; the existence of periodical solutions was verified observing the evolution of the system in the phase space projected to significant couples of variables of the system. In the simulations a critical summer condition, at the end of July, having a four-day period of absence of breeze was assumed.

d) A Poincarè section was constructed mapping the values of the concentration of the species, describing the state of the system, at a prefixed time for each simulated year; this time was chosen at the end of July, at the 6.00 a.m, corresponding to the last day of critical summer four-day period. It should be noted that a periodic solution of the dynamic systems, which in the phase space is described by a limit cycle, in a Poincarè section appears as a fixed point.

e) Response (or bifurcation) diagram, depicting the values at the fixed points of the more significant variables *vs.* the control parameter values, was constructed.

f) Critical values of control parameter were identified in correspondence of which a qualitative change of the state of the lagoon ecosystem was observed.

g) For one of these critical values simulations were carried out in which the maximum tidal flowrate was assumed as control paramenter and response diagrams were obtained.

3˙1. *Dynamic response of the lagoon ecosystem to variation of phosphorous external load*. – In fig. 1, a response diagram is shown; in the diagram the values, corresponding to the fixed points, of the vegetal species concentrations, integrated along the water column depth, and of the dissolved oxygen concentration at the bottom of the water column, *vs.* phosphorous load ($\mathrm{g/m^3\,s}$) are reported.

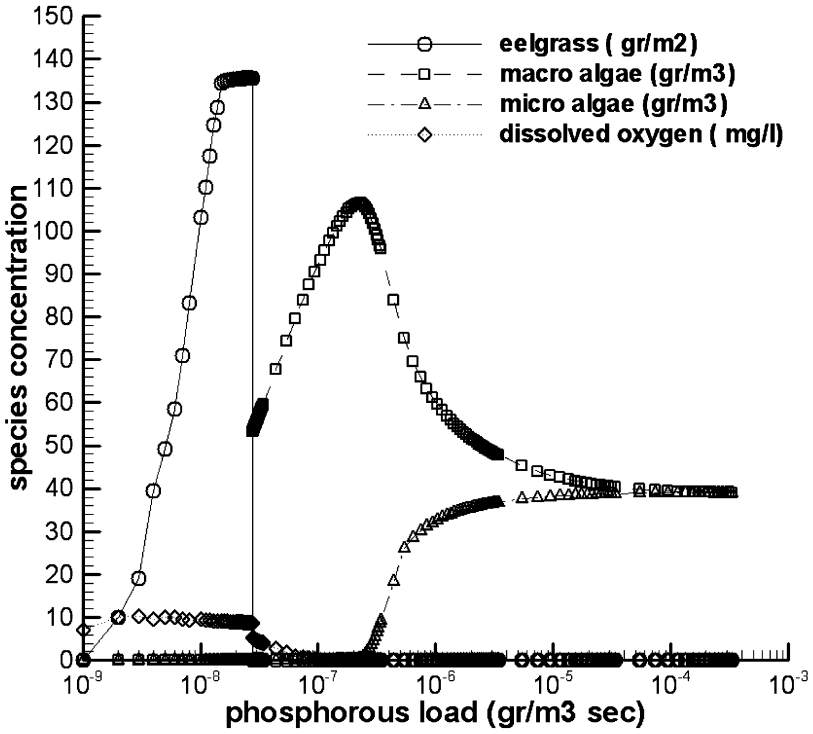

Fig. 1. – Response diagram: vegetal species concentration and dissolved oxygen *vs.* phosphorous load.

The figure shows that, varying the phosphorous load, different lagoon trophic conditions occur. These conditions are characterized by the dominance of specific vegetal species. In fact, in fig. 1, it is possible to identify three regions defined by the values of the control parameter q_{poimm}:

a) $q_{\text{poimm}} < 2.75 \times 10^{-8}\,\text{g/m}^3\,\text{s}$, region I: eelgrass is the only species present in lagoon; values of dissolved oxygen concentration are generally greater than 4 mg/l; no summer water anoxia occurs;

b) $2.75 \times 10^{-8} < q_{\text{poimm}} < 2 \times 10^{-7}\,\text{g/m}^3\,\text{s}$, region II: macroalgae is the only dominant species; for values of $q_{\text{poimm}} > 7 \times 10^{-8}$ the values of minimum summer dissolved oxygen concentration are practically null; this means that lagoon is subject each year to water anoxia phenomena;

c) $2 \times 10^{-7} < q_{\text{poimm}}\ \text{g/m}^3\,\text{s}$, region III: macroalgae and microalgae coexist. Also in this region the minimum summer dissolved oxygen concentration values are null denoting water anoxia phenomena.

In fig. 2 the response diagram, corresponding to the same fixed points of fig. 1, is shown. In the diagram the values of the following species *vs.* the phosphorous external load are shown: mean adsorbed phosphorous cocentration into sediments, mean dissolved phosphorous concentration in the water column, sulphate activity rate into sediment (calculated as the sulphide flow from the sediment to water column through the water

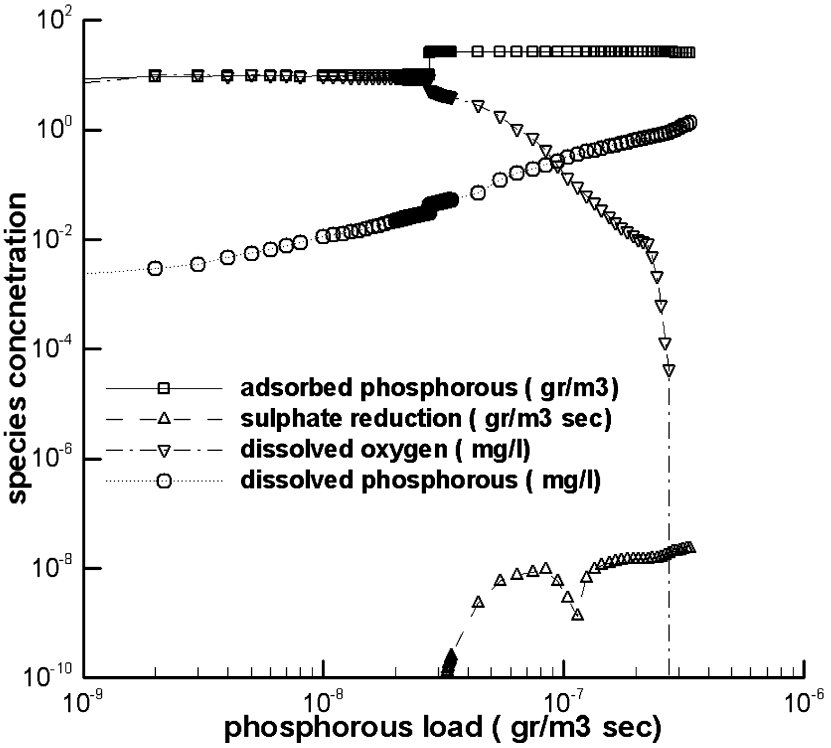

Fig. 2. – Response diagram: values of different species in the legend *vs.* phosphorous load.

sediment interface) and dissolved oxygen concentration at the bottom of the water column. The diagram of fig. 2 highlights the behaviour of these species within the three regions identified in fig. 1. In region I, dissolved and adsorbed phosphorous concentrations are lower than in the other regions, the dissolved oxygen concentration is higher, and further there is no appreciable sulphate attivity rate; in region II, the concentration of both dissolved and adsorbed phosphorous significantly increases respect to those of region I, the dissolved oxygen concentration decreases quickly with the increasing of control parameter, and the sulphate reduction rate assumes appreciable values. In region III, the phosphorous quantities increase further on, the dissolved oxygen concentration is equal to zero and the sulphate reduction rate reaches the maximum value.

The dynamics of the lagoon ecosystem, for an assigned value of the control parameter, can be analyzed in the phase space which describes the time evolution of the concentrations of two or more significant species.

In fig. 3 the phase plane refered to the adsorbed phosphorous concentration *vs.* the eelgrass concentration is shown.

Figure 3 is obtained by the calculated temporal series of the species concentrations. An example of these temporal series is shown in fig. 4. Figures 3 and 4 refer to the simulation with $q_{\mathrm{poimm}} = 5 \times 10^{-9}$. Figure 3 represents a typical behaviour of the ecosystem in the region I: after the transitory, a periodical solution is obtained, clearly evidenced by the existence of a limit cycle.

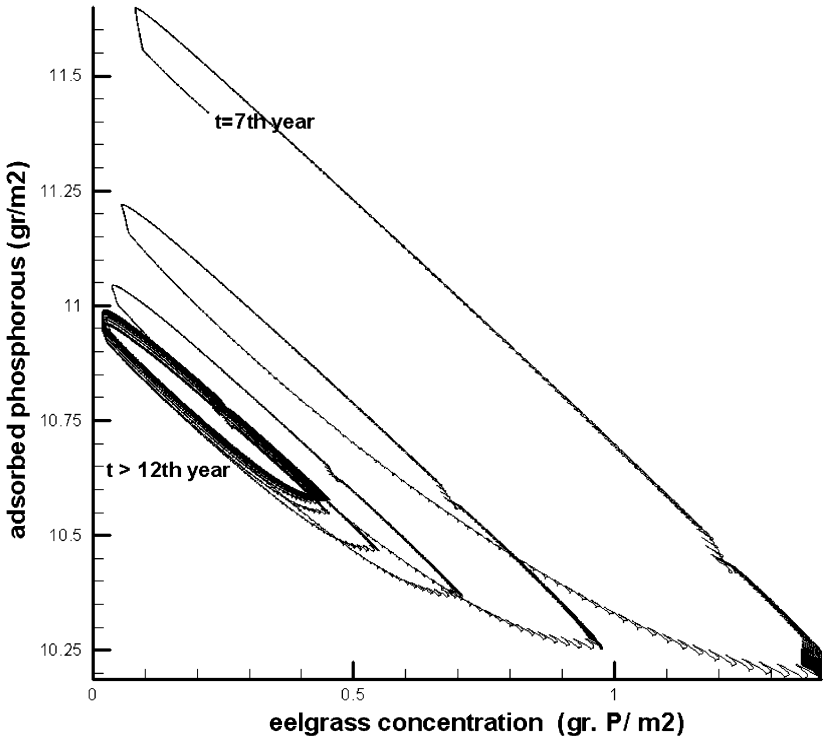

Fig. 3. – Phase plane: adsorbed phosphorous *vs.* eelgrass concentration ($q_{\mathrm{poimm}} = 5{\times}10^{-9}\,\mathrm{g/m^3}$).

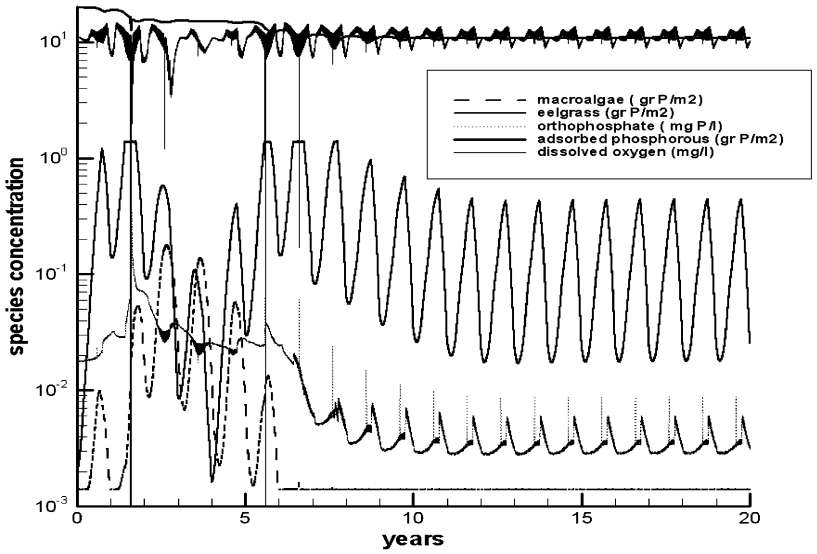

Fig. 4. – Significant species concentration *vs.* time ($q_{\mathrm{poimm}} = 5 \times 10^{-9}\,\mathrm{g/m^3}$).

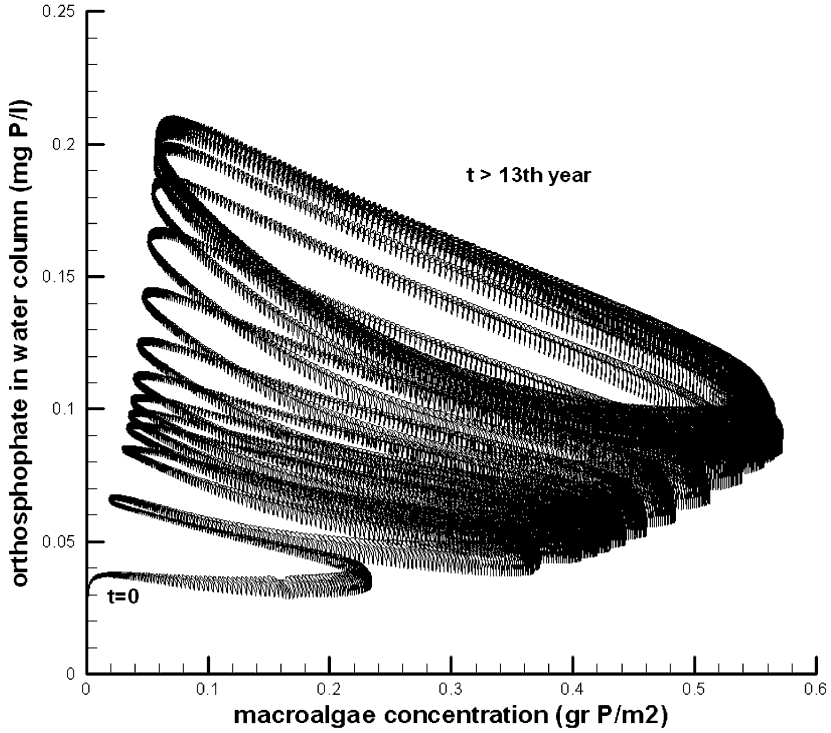

Fig. 5. – Phase plane orthophosphate *vs.* macroalgae ($q_{\mathrm{poimm}} = 5 \times 10^{-8}\,\mathrm{g/m^3}$).

It is possible to observe in fig. 3 that the higher values of the concentration of eelgrass correspond to lower values of adsorbed phosphorous concentration in sediments and vice versa: in fact eelgrass uptakes phosphorous from sediments, thus the quantity of adsorbed phosphorous reduces; at the end of the eelgrass life cycle the dissolved phosphorous produced by detritus mineralization is ready transformed in adsorbed phosphorus; the good oxygenation conditions of the environmental favourite the last process.

It should be noted (see figs. 4 or 2) that in the first region the orthophosphate concentration in water column is so low to prevent the floating algae growth.

The phase plane in fig. 5 shows the orthophosphate concentration in water column *vs.* macroalgae concentration; fig. 5 refers to a simulation in which a phosphorous load value within the region II was assumed ($q_{\mathrm{poimm}} = 5 \times 10^{-8}$); from fig. 5 it is possible to observe that, after the transitory, also in this case the trajectories collapse in a limit cycle. From the figure it is possible to observe that, in coherence with the macroalgae growth cycle, at higher macroalgae concentration values correspond lower orthophosphate concentration values and vice versa. In region II macroalgae is the dominant vegetal species.

This can be explained observing that in region II (see figs. 6 or 2) the orthophosphate concentrations in the water column, resulting from the balance between the phosphorous discharged into the lagoon and the one flushing from the lagoon to the sea, are high enough to allow the macroalgae growth, but not so high to support the microalgae growth. Furthermore eelgrass growth is inhibited by the shadowing due to the presence of macroalgae which find, at the top of the water column, the best light favourable conditions to grow.

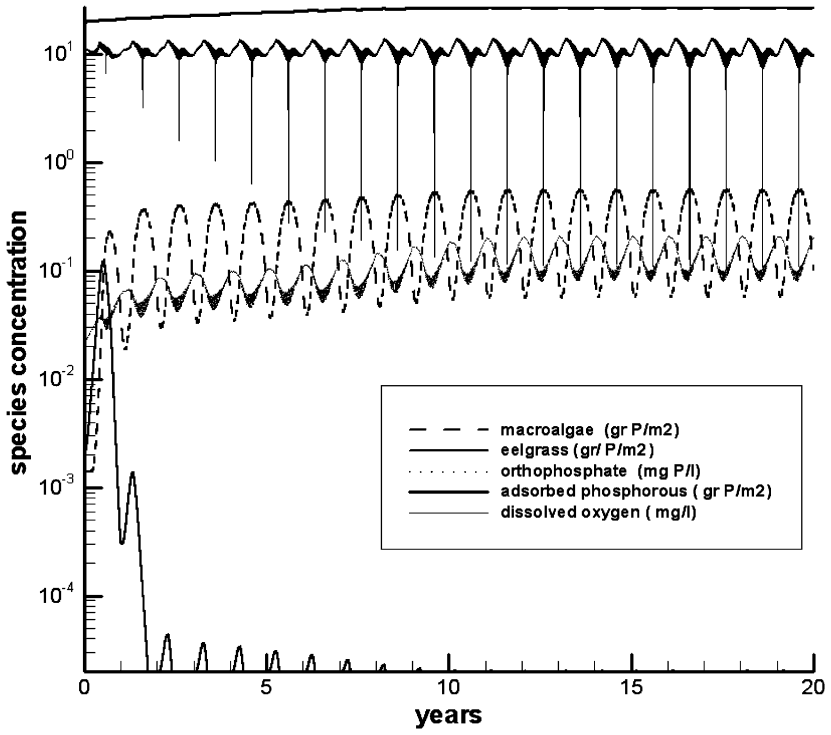

Fig. 6. – Significant species concentration *vs.* time ($q_{\mathrm{poimm}} = 5 \times 10^{-8}\,\mathrm{g/m^3}$).

From fig. 6 it can be observed that, starting from the 10th year, during the critical summer period when the wind speed falls down, the dissolved oxygen concentration at the water column bottom drops close to zero, *i.e.* summer water anoxia occurs.

Comparing fig. 6 with fig. 4, it is possible to observe that, even if the maximum quantities of vegetal organic carbon for eelgrass and macroalgae are about the same, the summer water anoxia occurs only in the case in which macroalgae are the dominant species. This result seems to demonstrate that a relationship exists between the kind of vegetal species and summer water anoxia in lagoons. A possible explanation can be found observing that the production of organic detritus is different in eelgrass and in macroalgae. In the case of rooted plants, as eelgrass, the organic detritus is produced at the end of the life cycle, in autumn, when leaves fall down; while floating species have a more rapid turn-over and therefore the organic production is more uniform during the life cycle (from the end of winter to autumn). Therefore, even if the floating macroalgae have about the same concentration of the eelgrass, the cycles of organic matter, phosphorous and sulphur are completely altered. More organic detritus is produced by floating algae, and more organic detritus settles and accumulates into sediments from the end of winter to the critical summer season. This determines a major oxygen requirement for the mineralization of organic matter and therefore more reducing conditions into sediments, which determinates a greater vulnerability of lagoon to summer water anoxia.

In fig. 7 the two limit cycles are shown related to, respectively, macroalgae and microalgae concentration *vs.* orthophosphate concentration in water column.

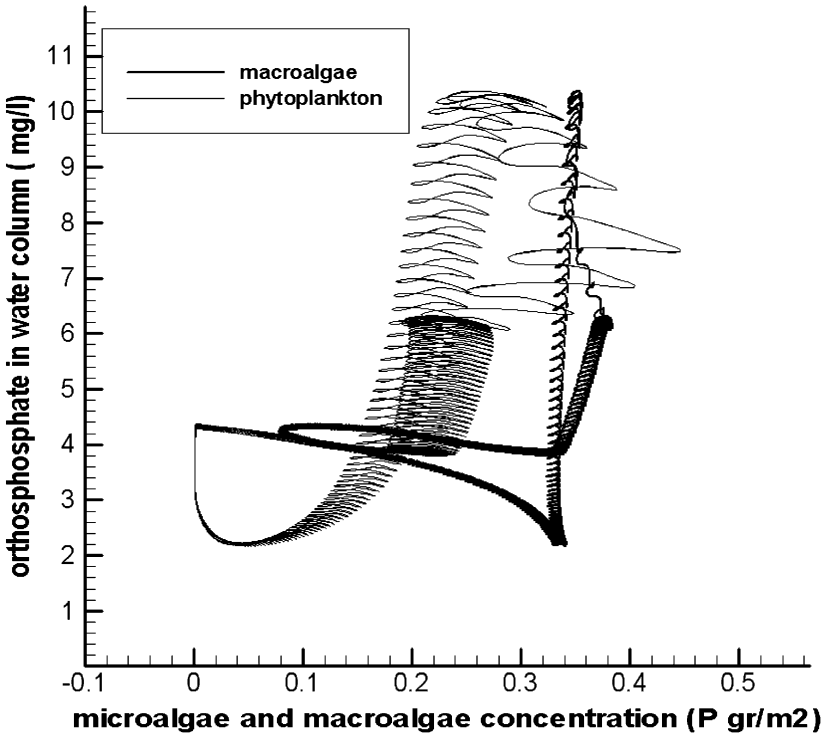

Fig. 7. – Phase plane orthophosphate *vs.* microalgae and/or macroalgae for $t > 15$ years ($q_{\mathrm{poimm}} = 5 \times 10^{-6}\,\mathrm{g/m^3}$).

Figure 7 refers to a phosphorous load value ($q_{\mathrm{poimm}} = 5 \times 10^{-6}$) within the region III. The two limit cycles present a very complex feature and no clear relation exists between the concentration of available phosphorous for algae growth and algae concentration, like in the cases of figs. 3 and 5. This is due to the fact that, during the entire summer period, frequent water anoxia occur also in the presence of breeze winds; such a quasi-permanent water anoxia condition determinates the release from sediment to water column of the adsorbed phosphorous in dissolved phosphorous. The phosphorous, released from sediments, affects the phosphorous balance in the water column masking the effect of algae uptakes.

Figure 1 showed that an abrupt change in vegetal species composition, from eelgrass to macroalgae, occurs within the small range of control parameter values: $2.7 \times 10^{-8} < q_{\mathrm{poimm}} < 2.8 \times 10^{-8}\,\mathrm{g/m^3\,s}$. In order to investigate this qualitative and "catastrophic" change in the ecosystem behaviour numerous simulations were carried out, in the previously indicated range, varying the control parameter of a quantity $\Delta q_{\mathrm{poimm}} = 2 \times 10^{-11}\,\mathrm{g/m^3\,s}$. Thus Poincarè sections were constructed mapping, at prefixed times with period $T = 1$ year, the values of the concentration of the species (see the description of point d)). In figs. 8 and 9 the most significant results of this analysis are shown. Figure 8 represents the Poincarè section related to eelgrass *vs.* macroalgae concentrations.

The letter A in fig. 8 indicates the point in which the trajectories describing the evolution of the state of the ecosystem in the first year of simulation intersects the

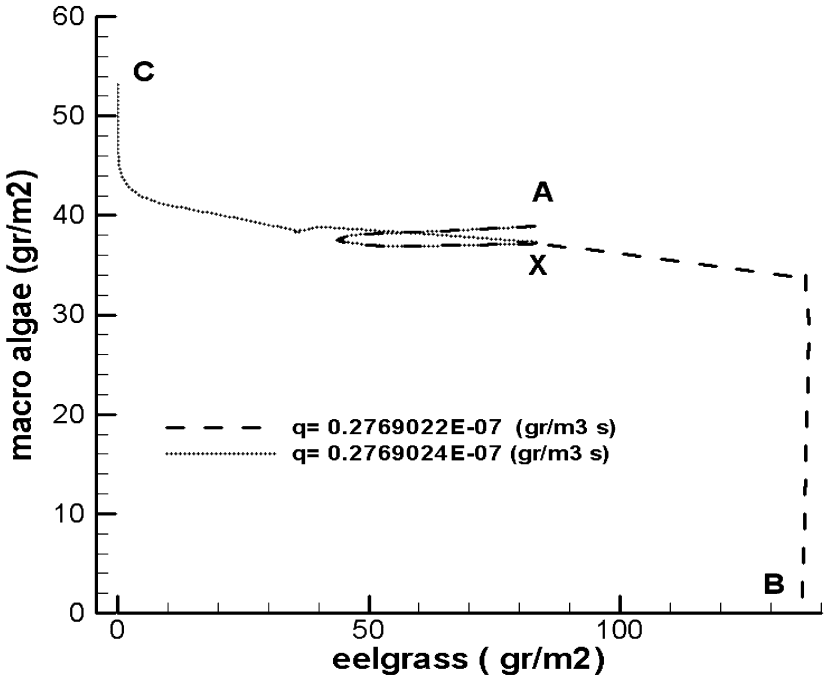

Fig. 8. – Poincarè section: eelgrass *vs.* macroalgae.

Poincarè section; the letters B and C in fig. 8 represent the fixed points, corresponding to limit cycles in the phase space, obtained by simulations in which two very close values of q_{poimm} were assumed ($q_{\text{poimm}} = 2.769022 \times 10^{-8}$ and $q_{\text{poimm}} = 2.769024 \times 10^{-8}$). The two curves in fig. 8 describe very close trajectories, but once in the point X indicated in the figure, the two curves move in opposite directions towards the respective fixed points.

This bifurcation behaviour is a direct consequence of the nonlinearity of the equation system representing the ecosystem. It should be deduced by fig. 8 that eelgrass and macroalgae are mutually exclusive; in fact the fixed point B represents a state of the ecosystem in which only eelgrass is present, whereas the fixed point C represents a state of the ecosystem in which macroalgae has completely replaced the eelgrass.

In order to complete the analysis, in fig. 9 the Poincarè section, constructed with the values of orthophosphate concentration *vs.* adsorbed phosphorous concentration, is shown; fig. 9 refers to the same simulations of fig. 8. The two fixed points B and C in fig. 9 refer to the same state of the ecosystems of the fixed points B and C in fig. 8. Point B in fig. 9 represents the state in which eelgrass is present, the dissolved phosphorous concentration is low, and the adsorbed phosphorous has been up-taken by eelgrass; while point C in fig. 9 represents a state of the system in which the concentration of dissolved phosphorous is high enough to support the macroalgae growth; further the adsorbed phosphorous concentration is in chemical equilibrium with the dissolved one.

3˙2. *Dynamic response of the lagoon ecosystem to change of lagoon hydrodynamics.* – The phosphorous load is not the only external forcing variable which can be assumed as control parameter. Change of hydrodynamics of the lagoon by tidal flow regulation

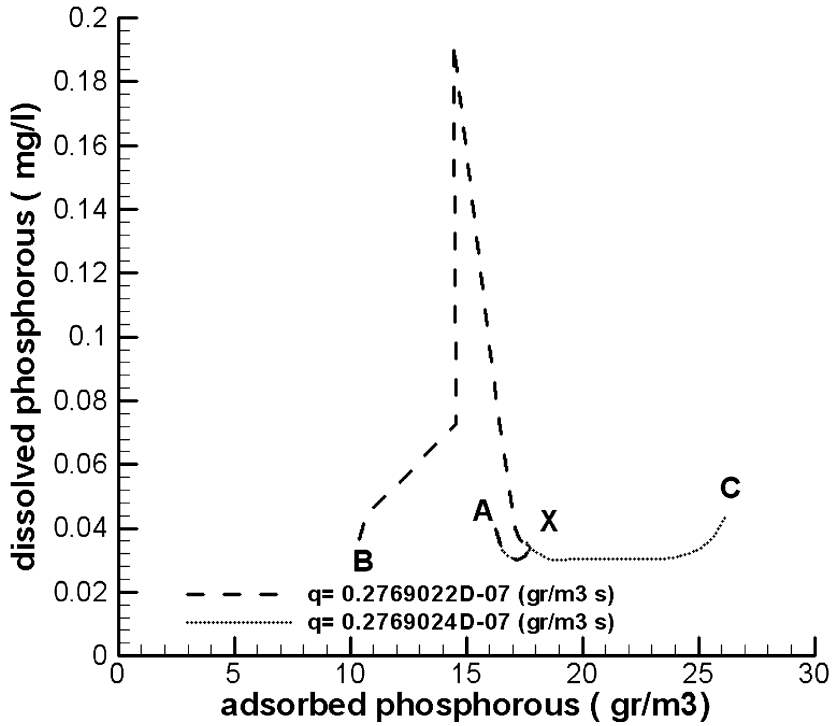

Fig. 9. – Poincarè section: dissolved *vs.* adsorbed phosphorous.

at the mouth of the channel connecting the lagoon to the sea, is one of the possible management strategies aimed at limiting eutrophication.

In fig. 10 a response diagram, obtained assuming the tidal maximum flowrate as control parameter, for a value of phosphorous load equal to 2.769023×10^{-8}, assumed as critical value of phosphorous load, is shown. From the figure it is possible to observe that the increase of tidal flow rate behind a critical value determinates an abrupt change from macroalgae to eelgrass. As a consequence of this vegetal species change, as shown in fig. 11, a higher value of dissolved oxygen at the bottom of the water column, a lower value of the internal phosphorous quantities and the absence of appreciable sulphate reduction activity occur.

This result shows that an increasing of the flushing in a lagoon due to a change of hydrodynamic conditions, can determine a substitution of the dominant vegetal species in a lagoon and an improving of the trophic state of the lagoon.

3˙3. *Model results versus the behaviour of a real lagoon.* – Although the results refer to a highly idealized scenarious, the dynamical analysis carried out provides a useful conceptual framework to understand the phenomena observed in real lagoons. In fact, in shallow Mediterranean coastal areas, phenomena such as vegetal species substitutions, anoxic crises and fish kills have often been recorded as a consequence of changes in external nutrient loads, hydrodynamic conditions or climate forcing factors; furthermore it has been also empirically observed that depending on the eutrophication level, these aquatic environments are colonized by different species of primary producers.

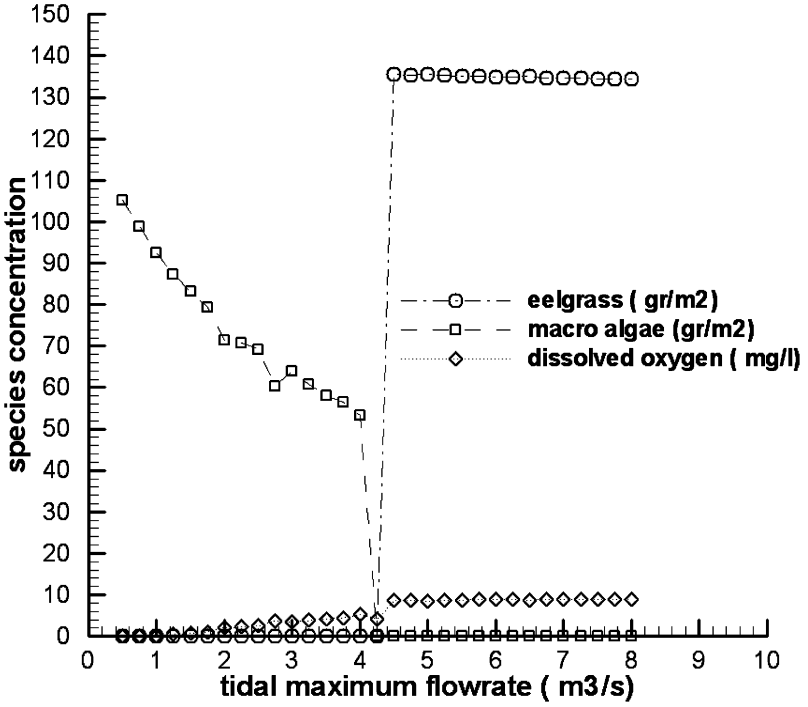

Fig. 10. – Vegetal species concentration *vs.* phosphorous load.

An example is the lagoon of Venice, that since the late 1980s has experienced strong environmental changes favouring the proliferation of macro algae, especially Ulva rigida C. Agardh, and limiting the presence of eelgrass, as Zostera. The abnormal growth of Ulva rigida triggered hypertrophic-dystrophic conditions and changed the natural equilibrium of the lagoon for over 20 years [16]. Under special conditions such as those encountered more frequently during the summer, anoxic crises with presence of hydrogen sulphide take place followed by sharp collapses in populations [17, 18].

In order to understand the reason for such environmental changes a lot of field studies have been carried out in the lagoon of Venice [19-22]. Some field studies have also recorded unexpected changes, from year to year, in the spatial distribution of the populations into the lagoon without significant variations of the external forcing factors [10]. This fact suggests that lagoon ecosystems exhibit non-linear dynamic behaviour where small variations of one or more forcing factors can determine an abrupt change between states of the system. The results discussed in the present paper support this hypothesis.

Up to date models have been constructed for a better understanding of the eutrophication phenomena in the lagoon of Venice and for forecasting the long-term evolution of such a ecosystem [23-28]. Even if these models differ one from the other, most of them offer a fair representation of eutrophication processes involved in shallow coastal areas, being able to capture the complex interaction between hydrodynamics and chemical and biological mechanisms.

However, due to their complexity, a systematic analysis of the dynamics of the ecosystem in relationship with variations of external control parameters is difficult to carry out; hence the analysis is confined to the investigation of only a specific state of ecosystem,

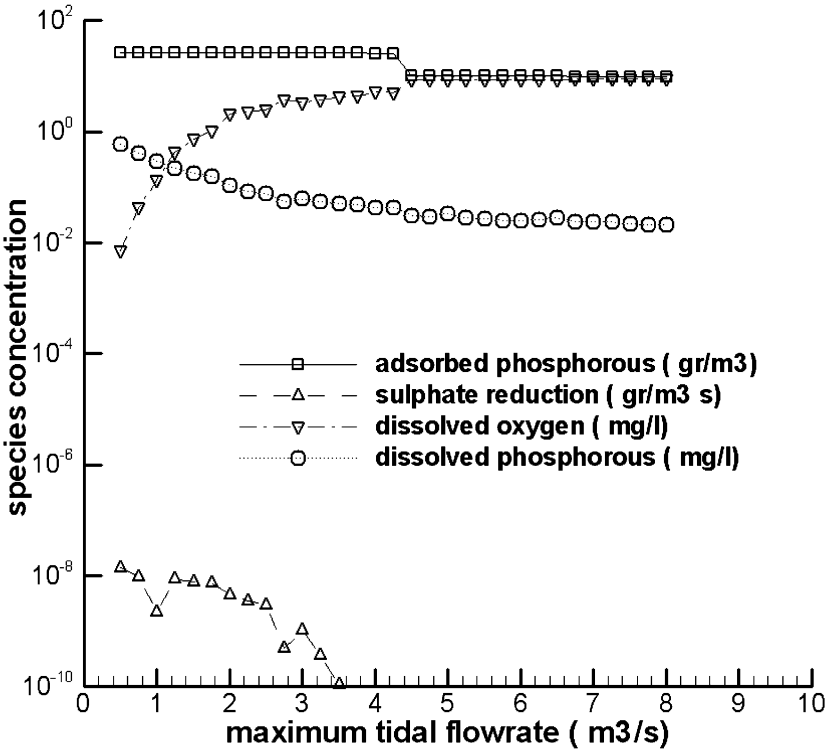

Fig. 11. – Species concentration *vs.* maximum tidal flowrate.

being practically impossible to determine the existence of both different stability regions of the ecosystem and the threshold values of external control parameters separating these different regions of stability.

These findings represent the main feature of the approach herein presented and have allowed the author to shed light aspects of lagoon ecosystem behaviours that to the author knowledge have not been emphasized before.

4. – Conclusion

The analysis of the dynamic behaviour of a lagoon ecosystem conducted by the eutrophication model has evidenced: a) the existence of different ranges of stability of the ecosystem depending on the value of the external phosphorous load and characterized by the dominance of a specific group of primary producers; b) in the ranges of values of the external phosphorous load where floating algae are dominant the ecosystem has a greater vulnerability to summer water anoxia. This can be justified on the bases of the different production modalities and rates of organic detritus of floating algae, micro and macroalgae, with respect to eelgrass; c) catastrophic bifurcations occur for critical values of the control parameters (phosphorous load and maximum tidal flow rate) which manifest with an abrupt substitution of eelgrass with macroalgae. This abrupt substitution can be explained observing that, once the othosphosphate concetrations in water column become enough high to support the macroalgae growth, the eelgrass growth is inhibited

by the shadowing due to the presence of macroalgae which find, at the top of the water column, the best light favourable conditions.

The dynamic analysis conducted has allowed the author to shed light into aspects of lagoon ecosystem behaviours that have often been observed in real shallow Mediterranean coastal area, as in the case of the lagoon of Venice, and therefore it provides a conceptual framework for a better understanding lagoon eutrophication phenomena that could be useful in management and recovery of these aquatic environments.

Appendix

External forcing factor: A: lagoon surface (km^2) 3.0; q: tidal flow rate (m^3/s) 4; breeze speed (m/s) 3.5.

$C_{\max}$: maximum eelgrass concentration (g C/l) = 100.

D_{mo}, D_{mn}, O2, H2S diffusion coefficients (m^2/s) 10^{-10}.

$\tilde{C}_{al}, \tilde{C}_{ph}, \tilde{C}_d, \tilde{C}_p, \tilde{P}_o, \tilde{H}, \tilde{O}$: species concentration at the lagoon outlet, equal to zero for entering tidal flow rates and equal to: C_{al}, C_{ph}, C_d, C_p, P_o, H, O, for going out tidal flow rates.

$$f_{al}(P_o) = P_o/(K_{poal} + P_o), f_{ph}(P_o) = P_o/(K_{poph} + P_o),$$
$$f_s(P_o, P_a) = (P_o + P_a)/(K_{pos} + P_o + P_a)$$

nutrient limiting factors.

$f(O) = O/(K_o + O)$ oxygen limiting factor.

$f(C_d) = C_d/(K_d + C_d)$ dissolved organic carbon limiting factor.

$$f(I) = (I/I_m) \cdot \sin(\pi \cdot \omega_y \cdot (t - t_s)) \sin(\pi \cdot \omega_d \cdot (t - t_s)) \cdot e^{-\gamma \cdot (h-z)}$$

light extinction.

$$f_{al,ph}(T) = {K_{tal,ph}}^{(T-T_{al,ph})},$$
$$f_m(T) = (T/T_m) \cdot e^{(1-(T/T_m))},$$

$f_\mu(T) = {K_{t\mu}}^{(T-T_\mu)}$ temperature limiting factors.

h: water column depth (m) 1.20.

h_s: sediment layer depth (m) 0.1.

K_a; aerobic adsorbing-desorbing phosphorus rate in sediment (s^{-1}) 2.5×10^{-6}.

K_d: half saturation constant (aerobic mineralization) (mg/l) 10.

K_{dal}, K_{dph}, K_{dm}: dissolved organic carbon production rate (s^{-1}) 10^{-7}, 10^{-6}, 5×10^{-8}.

K_H: reoxidation rate of hydrogen sulphide (s^{-1}) 4.2×10^{-6}.

K_o: half saturation constant limiting aerobic mineralization (mg/l) 0.3.

K_{pc}, K_{pmc} (mg/l ${PO_4}^-$)/(mg/l$C_{al,ph,d}$) 0.01.

K_p particulate organic in dissolved organic carbon rate (s^{-1}) 5×10^{-7}.

K_{pal}, K_{pph}, K_{pm} particulate organic carbon production rate (s^1) 10^{-7}, 10^{-6}, 5×10^{-8}.

K_{po} adsorbed-dissolved phosphorus half saturation constant (mg/l) 5×10^{-3}.

K_{poal}, K_{poph}, K_{pos} half saturation constants (mgPO_4/l) 0.02, 0.08, 0.01.

K_s organic carbon mineralization rate in anaerobic conditions (s^{-1}) 2.5×10^{-7}.

$K_{\gamma 1}$; $K_{\gamma 2}$; $K_{\gamma 3}$: $K_{\gamma 4}$ extinction light coefficients 0.06, 0.05, 0.005, 0.06.

$P_{ae} = P_{\max}(P_o/(P_o + K_{po}))$ equilibrium adsorbed phosphorous concentration.

$P_{\max}$: maximum adsorbed phosphorus concentration in sediments (mg/l) 700.
p_{or}: porosity = 0.8.
q_{pimm}, q_{dmm}, q_{poimm}: external loads of particulate and dissolved carbon and phosphorous.
r_{al}, r_{ph}, r_m: vegetal respiration rate (s^{-1}) 6×10^{-7}, 5×10^{-6}, 3×10^{7}.
α_{al} hydrodynamic factor 0.05.
α_p: anaerobic adsorbed phosphorus release rate in sediments (s^{-1}) 5×10^{-4}.
α_{por} equal to unity in the water column and equal to $(1 - p_{or})/p_{or}$ in sediments.
α_s (mg/l H_2S)/(mg/l C_d) 0.88.
α_μ (mg/l O2)/(mg/l $C_{al,ph,m}$) 2.66.
β_1, β_2: stochiometric constant.
$\gamma = K_{\gamma 1} C_{al} + K_{\gamma 2} C_{ph\gamma} + K_{\gamma 3} C_m + K_{\gamma 4} C_p$ light extinction factor.
μ_{cral}, μ_{crph}, μ_{crm}: vegetal growth rates.
μ_d: aerobic mineralization rate (s^{-1}) 6×10^{-6}, 5×10^{-5}, 3×10^{-6}.
ν_s: settling velocity of particulate organic carbon (m/s) $= 1 \times 10^{-6}$.
ν_t: turbulent diffusion coefficient and dispersion coefficient in sediments.
ω_y, ω_d, ω_m, ω_b: yearly, daily, tidal and breeze speed periods (d) 365,(h)24,12,24.

REFERENCES

[1] Cardoso P. G., Pardal M. A., Lillebo A. I., Ferreira S. M., Raffaelli D. and Marques J. C., *J. Exp. Mar. Biol. Ecol.*, **302** (2004) 233.
[2] Menèndez M. and Comìn F. A., *Estuar., Coast. Shelf Sci.*, **51** (2000) 215.
[3] Coffaro G. and Bocci M., *Ecol. Model.*, **102** (1997) 81.
[4] Moore Kenneth A. and Wetzel Richard L., *J. Exp. Mar. Biol. Ecol.*, **244** (2000) 1.
[5] Nelson Timothy A. and Lee Amorah, *Aquat. Bot.*, **71** (2001) 149.
[6] Peckol P. and Rivers J. S., *J. Exp. Mar. Biol. Ecol.*, **190** (1995) 1.
[7] Back H. K., *Ecol. Model.*, **65** (1993) 31.
[8] Coffaro G., Bocci M. and Bendoricchio G., *Ecol. Model.*, **102** (1997) 97.
[9] Raven J. A. and Taylor R., *Water, Air Soil Pollut.*, **3** (2003) 7.
[10] Sfriso A., Facca C., Ceoldo S. and Marcomini A., *Environ. Int.*, **31** (2005) 993.
[11] Carpenter S. R., Ludwing D. and Brock W. A., *Ecol. Appl.*, **9** (1999) 751.
[12] Collie J. S., Richardoson K. and Steele J. H., *Prog. Oceanogr.*, **60** (2004) 281.
[13] Cioffi F. and Gallerano F., *Appl. Math. Model.*, **30** (2006) 10.
[14] Cioffi F. and Gallerano F., *Appl. Math. Model.*, **25** (2001) 385.
[15] Wen Y. H., Vezina A. and Peters R. H., *Limnol. Oceanogr.*, **42** (1997) 45.
[16] Sfriso A., Facca C. and Ghetti P. F., *Mar. Environ. Res.*, **56** (2003) 617.
[17] Sfriso A., Marcomini A. and Pavoni B., *Mar. Environ. Res.*, **22** (1987) 297.
[18] Sfriso A., Pavoni B. and Marcomini A., *Sci. Total Environ.*, **80** (1989) 139.
[19] Marcomini A., Sfriso A., Pavoni B. and Orio A. A., *Eutrophication of the lagoon of Venice: nutrient loads and exchanges*, in *Eutrophic Shallow Estuaries and Lagoons*, edited by McComb A. J. (CRC Press, Boca Raton, Fl., USA) 1995, pp. 59–80.
[20] Sfriso A., Pavoni B., Marcomini A. and Orio A. A., *Estuaries*, **15** (1992) 517.
[21] Sfriso A. and Ghetti P. F., *Aquat. Bot.*, **61** (1998) 207.
[22] Sorokin Y. I., Sorokin I., Giovanardi O. and Dalla Venezia L., *Mar. Ecol. Prog. Ser.*, **141** (1996) 247.
[23] Bendoricchio G., Coffaro G. and De Marchi C., *Ecol. Model.*, **67** (1993) 221.
[24] Bocci M., *A mathematical model for studying Zostera noltii dynamics in the Venice lagoon*, in *The Venice Lagoon Ecosystem*, edited by Lasserre A. and Marzollo A., UNESCO (The Parthenon Publishing Group, Carnforth, UK) 2000, pp. 455–464.
[25] Solidoro C., Dejak C., Franco D., Pastres R. and Pecenik G., *Environ. Int.*, **21** (1995) 619.

[26] Solidoro C., Brando V. E., Dejak C., Franco D., Pastres R. and Pecenik G., *Ecol. Model.*, **102** (1997) 259.
[27] Solidoro C., Brando V. E., Franco D., Pastres R., Pecenik G. and Dejak C., *Environ. Model. Assess.*, **2** (1997) 65.
[28] Cioffi F. and Gallerano F., *Efficacia dei restringimenti fissi alle bocche di Porto della Laguna Veneta ai fini della difesa dell'acqua alta e loro impatto sui processi di eutrofizzazione, XXIX Convegno di Idraulica e Costruzioni Idrauliche, Trento, 7-10 Settembre 2004.*